Climate Dynamics
https://doi.org/10.1007/s00382-019-04669-5

The role of air-sea coupling in the downscaled hydroclimate projection over Peninsular Florida and the West Florida Shelf

Amit Bhardwaj[1,2] · **Vasubandhu Misra**[1,2,3]

Received: 25 September 2018 / Accepted: 4 February 2019

Abstract
A comparative analysis of two sets of downscaled simulations of the current climate and the future climate projections over Peninsular Florida (PF) and the West Florida Shelf (WFS) is presented to isolate the role of high-resolution air-sea coupling. In addition, the downscaled integrations are also compared with the much coarser, driving global model projection to examine the impact of grid resolution of the models. The WFS region is habitat for significant marine resources, which has both commercial and recreational value. Additionally, the hydroclimatic features of the WFS and PF contrast each other. For example, the seasonal cycle of surface evaporation in these two regions are opposite in phase to one another. In this study, we downscale the Community Climate System Model version 4 (CCSM4) simulations of the late twentieth century and the mid-twenty-first century (with reference concentration pathway 8.5 emission scenario) using an atmosphere only Regional Spectral Model (RSM) at 10 km grid resolution. In another set, we downscale the same set of CCSM4 simulations using the coupled RSM-Regional Ocean Model System (RSMROMS) at 10 km grid resolution. The comparison of the twentieth century simulations suggest significant changes to the SST simulation over WFS from RSMROMS relative to CCSM4, with the former reducing the systematic errors of the seasonal mean SST over all seasons except in the boreal summer season. It may be noted that owing to the coarse resolution of CCSM4, the comparatively shallow bathymetry of the WFS and the sharp coastline along PF is poorly defined, which is significantly rectified at 10 km grid spacing in RSMROMS. The seasonal hydroclimate over PF and the WFS in the twentieth century simulation show significant bias in all three models with CCSM4 showing the least for a majority of the seasons, except in the wet June-July-August (JJA) season. In the JJA season, the errors of the surface hydroclimate over PF is the least in RSMROMS. The systematic errors of surface precipitation and evaporation are more comparable between the simulations of CCSM4 and RSMROMS, while they differ the most in moisture flux convergence. However, there is considerable improvement in RSMROMS compared to RSM simulations in terms of the seasonal bias of the hydroclimate over WFS and PF in all seasons of the year. This suggests the potential rectification impact of air-sea coupling on dynamic downscaling of CCSM4 twentieth century simulations. In terms of the climate projection in the decades of 2041–2060, the RSMROMS simulation indicate significant drying of the wet season over PF compared to moderate drying in CCSM4 and insignificant changes in the RSM projection. This contrasting projection is also associated with projected warming of SSTs along the WFS in RSMROMS as opposed to warming patterns of SST that is more zonal and across the WFS in CCSM4.

1 Introduction

Peninsular Florida (PF) has a rapidly growing population of the elderly (Smith 2005; Carlson 2012) and require reliable estimates of regional change in order to determine appropriate adaptation and mitigation strategies to a changing climate. The regional climate projection although of great societal relevance is however elusive. The difficulty primarily arises from the uncertainties of the interactions of the large-scale with the local processes of the regional climate. The exorbitant resources required to run very high-resolution

✉ Amit Bhardwaj
abhardwaj@fsu.edu

1 Center for Ocean-Atmospheric Prediction Studies, Florida State University, Tallahassee, FL, USA

2 Florida Climate Institute, Florida State University, Tallahassee, FL, USA

3 Department of Earth, Ocean and Atmospheric Science, Florida State University, Tallahassee, FL, USA

Global Circulation Models GCMs; (e.g. cloud and or ocean eddy resolving scales) prohibit their regular deployment yet for routine climate model integrations (Shukla et al. 2009; Kirtman et al. 2012, 2017; Jia et al. 2014; Siqueira and Kirtman 2016; Laurindo et al. 2018). Nonetheless, some of these recent studies demonstrate the ongoing effort to raise the resolution of the models significantly from their current values for climate integrations. The alternative has been to regionalize the GCMs with either statistical or Dynamical Downscaling (DD) methods. Neither of these two methods is known to have a clear superiority over the other (Hewitson and Crane 1996; Wilby and Wigley 1997). In this study, we compare two sets of DD simulations of the current and future climate over PF with the corresponding simulations from the driving GCM. The intent of this paper is to motivate the use of high-resolution coupled ocean–atmosphere models for regional climate projections for PF and surrounding oceans. In order to accomplish this task, we compare the simulations of the current climate and projections of the future climate between the fine and coarse resolution models. Furthermore, we also highlight the differences in the model integrations between coupled ocean–atmosphere and uncoupled atmosphere models at the fine spatial resolution scales. The benefit of resolving air-sea coupling in DD

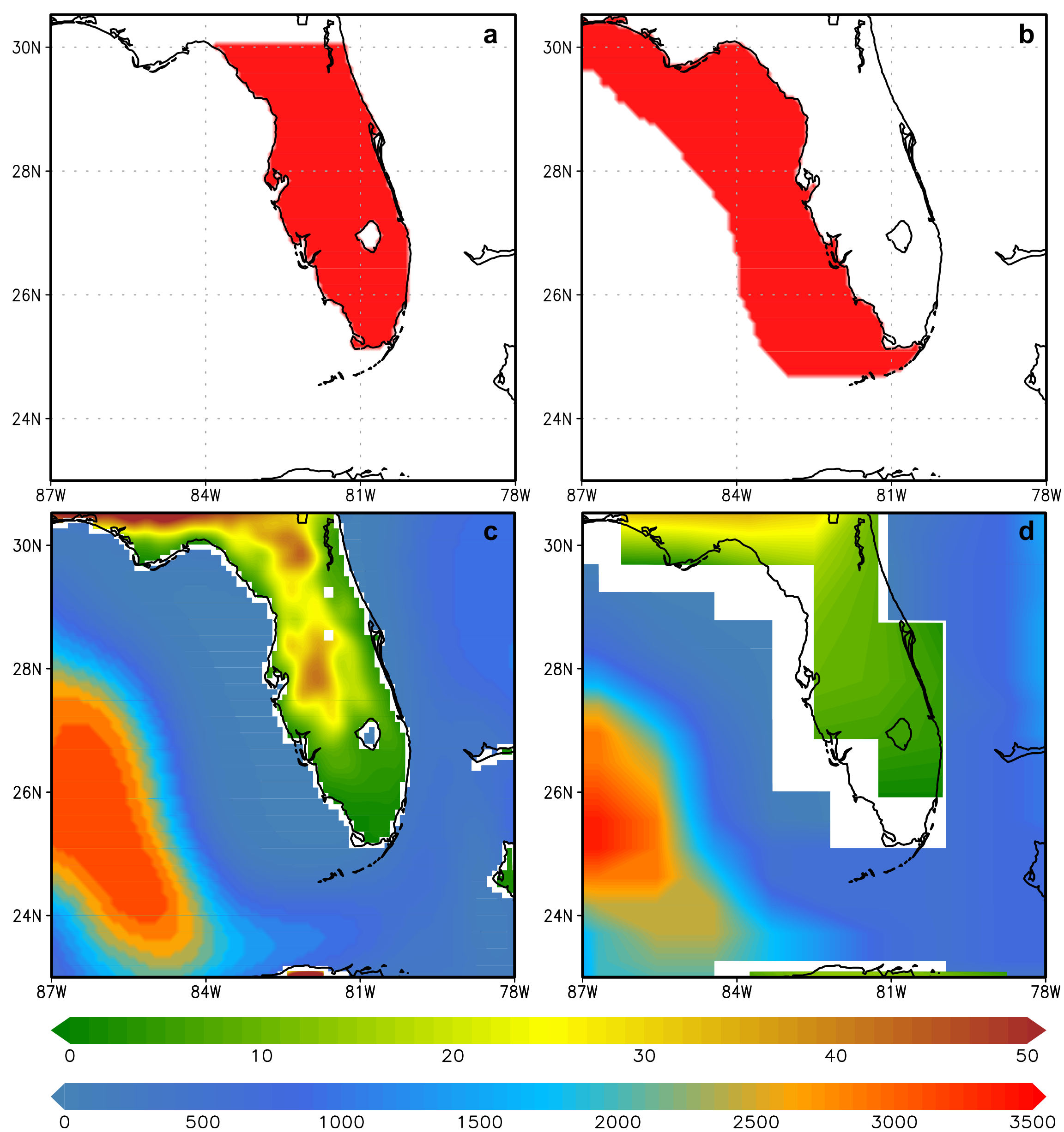

Fig. 1 The mask for a Peninsular Florida (PF), and b West Florida Shelf (WFS). The ocean bathymetry and terrestrial topography used in c RSMROMS (regional climate model used in the study) and d the driving general circulation model (CCSM4). The units are in meters

is that ocean rectification can potentially lead to improved simulation of the atmospheric climate of the region (Misra and Mishra 2016; Misra et al. 2016).

The terrestrial hydroclimate of PF shows a distinct seasonality (Fig. 1a; Misra and Dirmeyer 2009; Misra and DiNapoli 2012; Misra and Mishra 2016; Misra et al. 2017). For example, Misra and Dirmeyer (2009) indicate the important role of evaporation on precipitation in the summer season, which is significantly diminished in the winter season. Misra et al. (2017) indicate that the seasonal evolution in to the wet, summer season over PF coincides with the gradual warming of the Intra-Americas Seas that eventually enhances the moisture flux into PF to initiate the onset of the rainy season. Misra and Mishra (2016) also find that the seasonal maturity of the warm coastal Florida Current also contributes to increased moisture flux over PF through the associated warming of the coastal SST. Furthermore, Liu et al. (2012, 2013, 2015) indicate that all climate models in the Coupled Model Intercomparison Project 5 (CMIP5) did not adequately resolve the Loop Current system leading to a systematic cold bias in the IAS SST. Therefore, examining the role of air-sea coupling on DD of GCM climate simulations over PF would be interesting from aspects of assessment of the current climate simulation and future climate projection.

The West Florida Shelf (WFS; Fig. 1b) is described as being oligotrophic (Steidinger 1975; Dixon et al. 2014). However, it supports significant commercial and recreational fisheries (https://www.st.nmfs.noaa.gov/commercial-fisheries/). Furthermore, WFS also shows periods of harmful algal blooms (Heil et al. 2014; Weisberg et al. 2016a, b). In fact, Weisberg et al. (2016a, b) from their analysis of numerical simulations reveal that the interactions of the Loop Current with the shelf slope can lead to anomalous upwelling, which leads to renewal of inorganic nutrients and foster potential harmful algal blooms.

We will be focusing on two regions in terms of validation of the model simulation of the current climate and projection of the future climate, which are over terrestrial PF (Fig. 1a) and over the WFS (Fig. 1b). These regions assume significance from the obvious choices of PF and WFS being significant habitat for human population and marine resources, respectively. Furthermore, our choices of these two subregions are dictated by the improved bathymetry of the WFS region in the regional climate model used for this study (Fig. 1c), which we would anticipate could cause significant changes to the climate simulation from the driving GCM, if air-sea coupling with shallower ocean is playing a critical role in the region. In addition, the PF region is an obvious choice for further analysis given the earlier finding of Misra and Mishra (2016) that terrestrial hydroclimate over PF could be influenced by air-sea coupling in the surrounding oceans. Furthermore, some of the GCM studies indicate that improving the simulation of the Gulf Stream leads to large-scale structural changes in mean rainfall, especially along the eastern US (Kirtman et al. 2012). There is also some evidence to suggest that resolved oceanic mesoscale features can affect the upper atmospheric features through non-linear interactions (Kirtman et al. 2017).

In the following section, we provide a description of the model experiment set up along with a brief description of the models used in the study. The results from the coupled and uncoupled DD along with comparison of the corresponding GCM simulations and observations for the late 20th and mid twenty-first centuries are discussed in Sect. 3 a and b respectively. The concluding remarks are discussed in Sect. 4.

2 Experiment set up and model description

The DD of the twentieth century historical simulation and the corresponding projected climate simulation using the Reference Concentration Pathway (RCP) 8.5 emission scenario (van Vuuren et a. 2011) of the Community Climate System Model version 4 (CCSM4; Gent et al. 2011) is conducted in this study. The DD to 10 km grid spacing is centered over PF (Fig. 1c) and conducted over a time period of 1986–2005 for the twentieth century and 2041–2060 for the twenty-first century using corresponding CCSM4 simulations as the lateral boundary conditions for the regional models.

One of the two DD was conducted with the Regional Spectral Model (RSM; Kanamitsu et al. 2010 and; Misra et al. 2017), which is a regional atmosphere model routinely run for regional climate simulations with prescribed SST (Chan and Misra 2011; Misra et al. 2013). The other DD was conducted with the RSM-Regional Ocean Modeling System (RSMROMS; Li et al. 2012; Misra et al. 2017), which is the regional coupled ocean–atmosphere system. The atmospheric component, RSM, is identical for both the uncoupled and coupled DD integrations. The coarse resolution of CCSM4 relative to RSMROMS is apparent in the land orography and ocean bathymetry features of the domain shown in Fig. 1c, d. In CCSM4, the coarse coastlines manifest in jagged edges of the coastlines and the topography over PF is mostly below 10 m (Fig. 1d) when in RSMROMS it is over 30 m at least from northern panhandle to central Florida and the coastlines conform more to realism (Fig. 1c). Similarly, the WFS is broad and closely hugs the western Florida coastline in RSMROMS (Fig. 1c) unlike in CCSM4 (Fig. 1d). Likewise, the Sigsbee Deep, the deepest part of the Gulf of Mexico is more accurately depicted in the ocean bathymetry of RSMROMS (Fig. 1c) than in CCSM4 (Fig. 1d), especially as it extends closer to Cuba. It is disturbing to note that in CCSM4 (Fig. 1d), the white spaces are neither ocean or land points. This is because of the mis-match in the resolutions of the ocean and atmosphere component models in CCSM4, which the flux coupler is able to easily handle and allow the model to integrate through, despite these so called "orphaned" grid points. Therefore, the practical utility of climate projections from such coarse grained climate models for a region like the WFS or south Florida can be limited.

The RSM, following Juang and Kanamitsu (1994) has 28 terrain following vertical co-ordinate system of sigma ($\sigma = p/p_s$; where p_s is surface pressure) and is based on the primitive equations. The RSM is discretized using the spectral method of double sine–cosine series with wall boundary conditions (Tatsumi 1986). It uses the semi-implicit time integration scheme. RSM uses the relaxed Arakawa-Schubert scheme (Moorthi and Suarez 1992) for deep convection, shallow convection scheme follows Tiedtke (1983), Hong and Pan (1996) for boundary layer processes, Zhao and Carr (1997) for the cloud scheme, land surface processes are parameterized following Ek et al. (2003), gravity wave drag is parameterized following Alpert et al. (1988), shortwave and longwave radiation follows from Chou and Lee (1996) and Chou et al. (1999), respectively. Similarly, the Regional Ocean Model System (ROMS) version 3.0 in RSMROMS uses 30 vertical levels. This is a stretched terrain following (S) co-ordinate on a horizontal staggered Arakawa-C grid (Haidvogel et al. 2000; Shchepetkin and McWilliams 2005). The mixing scheme is a local closure scheme following the level 2.5 turbulent kinetic energy equations (Mellor and Yamada 1982) and generic length scale parameterization of Umlauf and Burchard (2003). The boundary layer formulation follows Large et al. (1994), which is a nonlocal closure scheme based on the K-profile. The horizontal grids in RSM and ROMS are identical, which avoids interpolation of the variables exchanged between the two components at the coupling interval.

The lateral and initial boundary conditions for the present and future climate simulations for both RSM and RSMROMS are from the corresponding CCSM4 simulation. The atmospheric grid resolution of CCSM4 is 1.25° × 0.9°. The zonal grid spacing in the ocean component of CCSM4 is 1.11° and the meridional grid spacing varies from 0.27° near the equator to 0.54° at 33°N/S. Thereafter, the meridional grid spacing is held constant at that resolution at higher latitudes. The prognostic variables of the CCSM4 are linearly interpolated for initial and lateral boundary conditions for RSM and ROMS at 6-h and monthly intervals respectively. We neglect the first year of the RSMROMS integration in consideration of spin-up issues of the upper ocean. Therefore, we use the remaining 20 years of the RSMROMS and RSM simulations of the current (1986–2005) and future (2041–2060) climate for analysis with corresponding period from the CCSM4 integration used for comparison. The validation datasets to validate the twentieth century simulations are indicated in Table 1.

3 Results

3.1 Simulation of the current (1986–2005) hydroclimate

In this first sub-section of the "Results" Section we will analyze the model simulations for the 20 years of the current climate (1986–2005). In the subsequent sub-section, we will inter-compare the climate projections of the future climate (2041–2060).

3.1.1 Surface temperature

The seasonal cycle of observed SST is robust in the domain, especially over the WFS, where the temperatures are well below 23 °C in the December-January-February (DJF; Fig. 2a) season, with some warming in southern parts of the shelf in the subsequent season of March-April-May (MAM; Fig. 2b). The observed SST reaches a peak in the summer season of June-July-August (JJA; Fig. 2c) when the temperature reaches over 28 °C across the WFS (Fig. 2c) and then gradually drops in magnitude in the following September-October-November (SON) season to around 26 °C (Fig. 2d).

Table 1 Verification datasets for model validation

	Variable	Name of dataset (Acronym used to identify dataset)	Spatial resolution of dataset	Temporal resolution of dataset	Available time period	Source
1	Precipitation	TRMM-3B43 (TRMM)	0.25° × 0.25°	Daily	1998–2015	Huffman et al. 1995; 1997; Adler et al. 2000
2	Ocean surface temperature	SODAv2.2.4 (Simple Ocean Data Assimilation)	0.25° × 0.4° × 40 Levels	Monthly	1958–2001	Carton, and Giese, (2008)
3	Land surface temperature	MERRA-2	0.5° × 0.625°	Daily	1979-present	Suarez and Bacmeister (2015)
4	Upper air variables and surface evaporation	MERRA-2	0.5° × 0.625°	Daily	1979-present	Suarez and Bacmeister (2015)

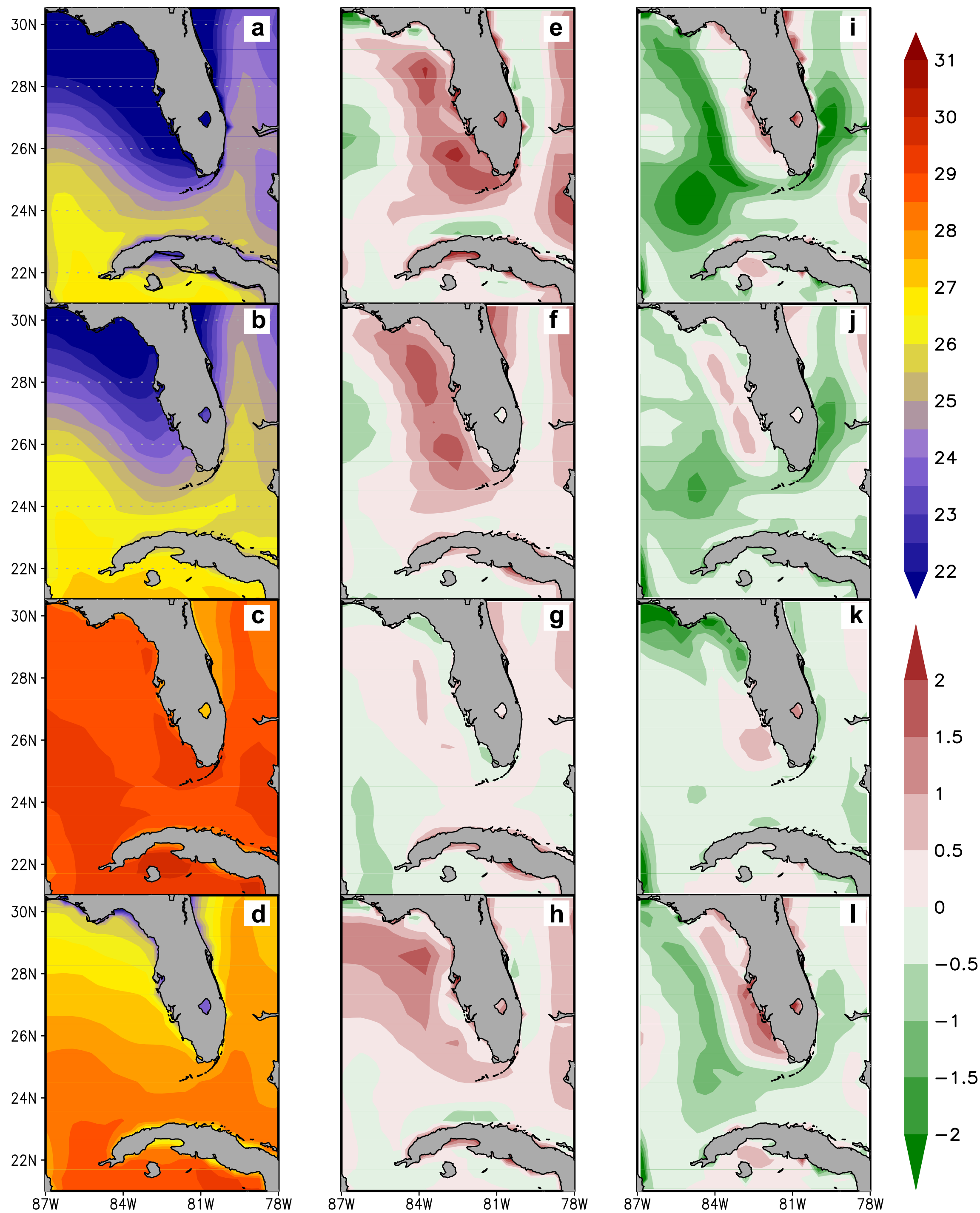

Fig. 2 The climatological seasonal mean observed SST for a December-January-February (DJF), b March-April-May (MAM), c June-July-August (JJA), and d September-October-November (SON) seasons. The corresponding systematic errors of the seasonal mean SST from e–h CCSM4, and i–l RSMROMS; for e, i DJF; f, j MAM; g, k JJA, and h, l SON seasons. The units are in °C

This is not surprising given that earlier studies have recognized that the seasonal cycle of SST variations in the WFS responds to corresponding seasonal changes in the surface radiative and enthalpy flux forcing alongside subsurface forcing of ocean circulation changes (Tolbert and Salsman 1964; Yang and Wisberg 1999; He et al. 2003; Weisberg et al. 2004; Liu and Weisberg 2012). The relatively rapid warming of the waters from the boreal winter to the summer season in both the models is reasonably captured (Fig. 2e–g). The warm bias over the WFS in the CCSM4 simulation is however predominant across all four seasons of the year (Fig. 2e–h). The warm bias over the WFS is considerably reduced in the RSMROMS (Fig. 2i–l) relative to CCSM4. This is also ascertained by the lower Root Mean Square Error (RMSE) in the RSMROMS simulation computed in Table 2. We observe that the differences in RMSE between the two model simulations range from about 0.74 °C (in MAM season) to about 0.15 °C (in SON season) with the exception that in the JJA season the RMSE in CCSM4 is lower than in RSMROMS (Table 2). We argue that despite the comparatively small difference in the RMSE between the two model simulations, it is still a sign of major improvement for RSMROMS in the majority of the seasons because CCSM4 produces smoother fields owing to its coarse resolution and therefore will tend to exhibit low RMSE (Wilks 2011). It may be noted that SST from the CCSM4 integration is prescribed for the uncoupled RSM integration.

Similarly, the RMSE of the land surface temperature over PF exhibits lower values for RSMROMS relative to CCSM4, except in the season of JJA. Here, the range of difference in the RMSE between the two models is from 1.55 °C (in the DJF season) to 0.2 °C (in the JJA season). Again, the fact that the RSMROMS grid resolution is about an order of magnitude higher than that of CCSM4 over land further attests to the significance of this improvement in the simulation of the land surface temperature over PF in the majority of the seasons.

In summary, RSMROMS shows an improvement of the seasonal surface temperature over the WFS and PF compared to CCSM4, which is significant considering the resolved mesoscale gradients by RSMROMS. The clear benefit of resolving the shallow bathymetry of the WFS in RSMROMS manifests with generally a lower RMSE in the seasonal SST over WFS relative to CCSM4.

3.1.2 Surface precipitation

The observed seasonal cycle of precipitation is also equally robust as the SST in the region with widespread drying over both terrestrial PF and over the WFS in DJF (Fig. 3a) and MAM (Fig. 3b) seasons, which is followed by the wettest JJA season (Fig. 3c) before the land-based precipitation diminishes in the SON season (Fig. 3d). In fact, Misra et al. (2017) indicate that the onset of the rainy season over PF is rather dramatic with rain rates increasing by a factor of 3 on the day of the onset. In relation to the observed seasonal mean precipitation, the systematic errors in all three models are comparatively large (Fig. 3e–p; Table 3). In the DJF season, the wet bias over PF is severe and Table 3 indicates that it increases from CCSM4 (Fig. 3e) to RSMROMS (Fig. 3i) with RSM displaying the largest bias (Fig. 3m). Similarly, the dry bias over the southern part of WFS is also far more severe in RSM (Fig. 3m) in relation to the other two models (Table 3).

The MAM season also shows a similar feature of RSM showing the most severe wet bias over PF and over the southern part of the WFS (Fig. 3n), followed by the dry bias over PF in the RSMROMS (Fig. 3j) with the least bias over PF in the CCSM4 simulation (Fig. 3f; Table 3). Furthermore, the dry bias over the WFS in the MAM season is comparable in both CCSM4 (Fig. 3f) and RSMROMS (Fig. 3j) but is least in the RSM simulation (Fig. 3n). This is because in RSM, parts of southern WFS have dry bias that compensates for the wet bias in the rest of the WFS to an extent (Table 3).

The bias changes sign in the JJA season with all three models displaying near comparable dry systematic errors over the WFS and PF (Fig. 3g, k, o; Table 3). The wet bias over PF returns in the SON season with comparable errors in all three models (Fig. 3h, i, p; Table 3). It may be noted that systematic errors of precipitation in the SON season is the least for all three models compared to the other three seasons (Table 3).

In terms of surface precipitation over the WFS and PF, CCSM4 displays the least RMSE compared to either RSMROMS or RSM except in the wet JJA season. In the JJA season, RSMROMS shows the least RMSE over PF. The improvement in the SST simulation in RSMROMS could be one of the reasons for the improvement in surface precipitation over PF. As Misra and Mishra (2016) noted there is stronger influence of the surrounding oceanic SST on the JJA precipitation over PF, while in other seasons rainfall from frontal and other large-scale systems, which could be sensitive to the boundary forcing is potentially important. Furthermore, the systematic improvement of seasonal precipitation across all four seasons over PF and

Table 2 RMSE of SST over West Florida Shelf (WFS) and land surface temperature (TS) over Peninsular Florida (PF)

	DJF		MAM		JJA		SON	
	CCSM4	RSMROMS	CCSM4	RSMROMS	CCSM4	RSMROMS	CCSM4	RSMROMS
SST (WFS)	1.31	1.16	1.30	0.56	0.36	0.96	0.98	0.83
TS (PF)	2.38	0.83	0.88	0.45	0.61	0.81	0.91	0.83

Units in °C

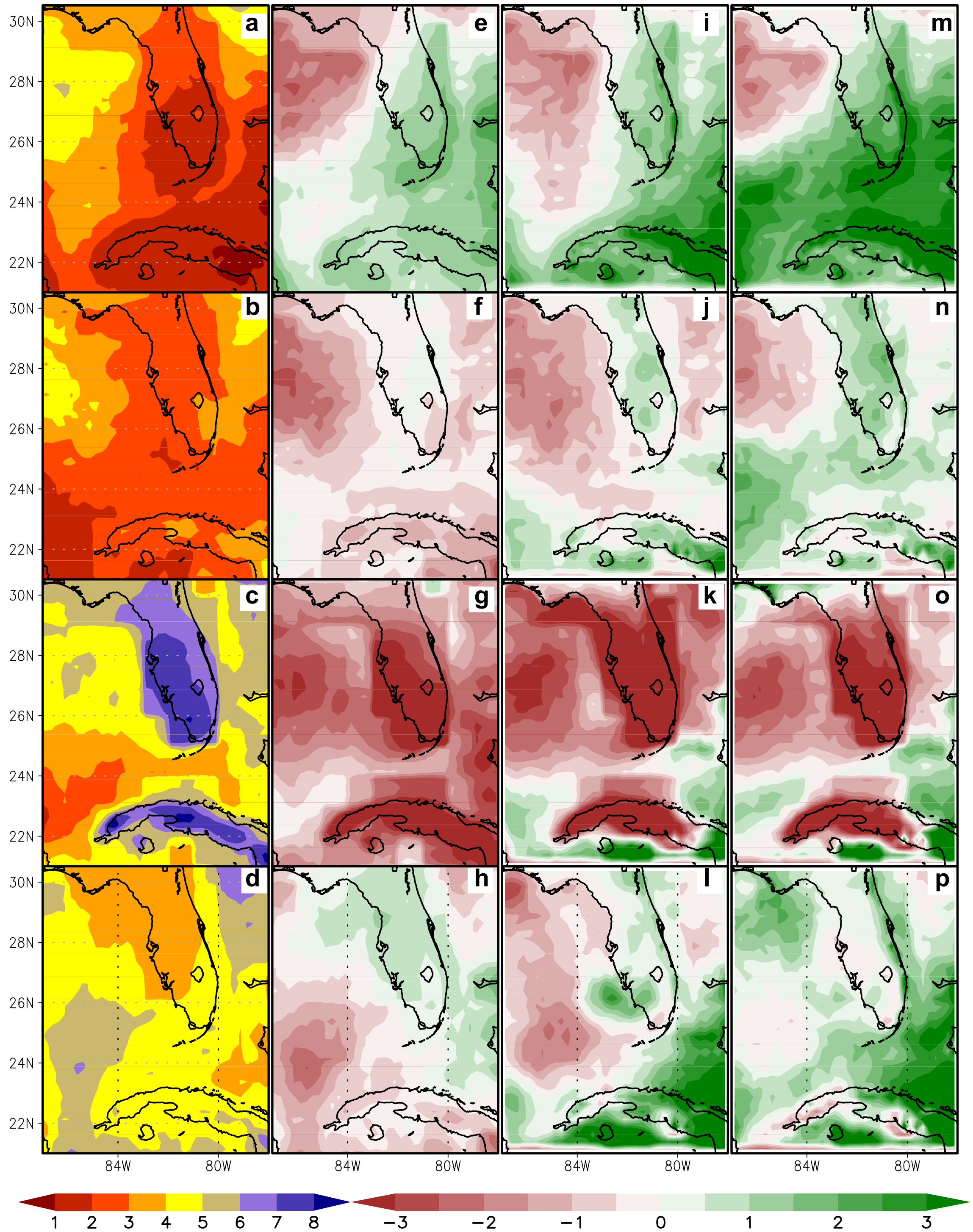

Fig. 3 The climatological seasonal mean observed precipitation for a DJF, b MAM, c JJA, and d SON seasons. The corresponding systematic errors from e–h CCSM4, i–l RSMROMS, and m–p RSM for e, i, m DJF; f, j, n MAM; g, k, o JJA; and h, l, p SON seasons. The units are in mm day^{-1}

Table 3 RMSE of precipitation over West Florida Shelf (WFS) and over Peninsular Florida (PF)

	DJF			MAM			JJA			SON		
	CCSM4	RSMROMS	RSM	CCSM4	RSMROMS	RSM	CCSM4	RSMROMS	RSM	CCSM4	RSMROMS	RSM
PF	0.93	1.17	1.59	0.30	0.90	1.10	3.12	2.74	3.13	0.67	0.73	0.69
WFS	1.34	1.20	1.61	0.92	1.0	0.71	2.57	2.71	2.23	0.56	0.76	1.01

Units in mm day^{-1}

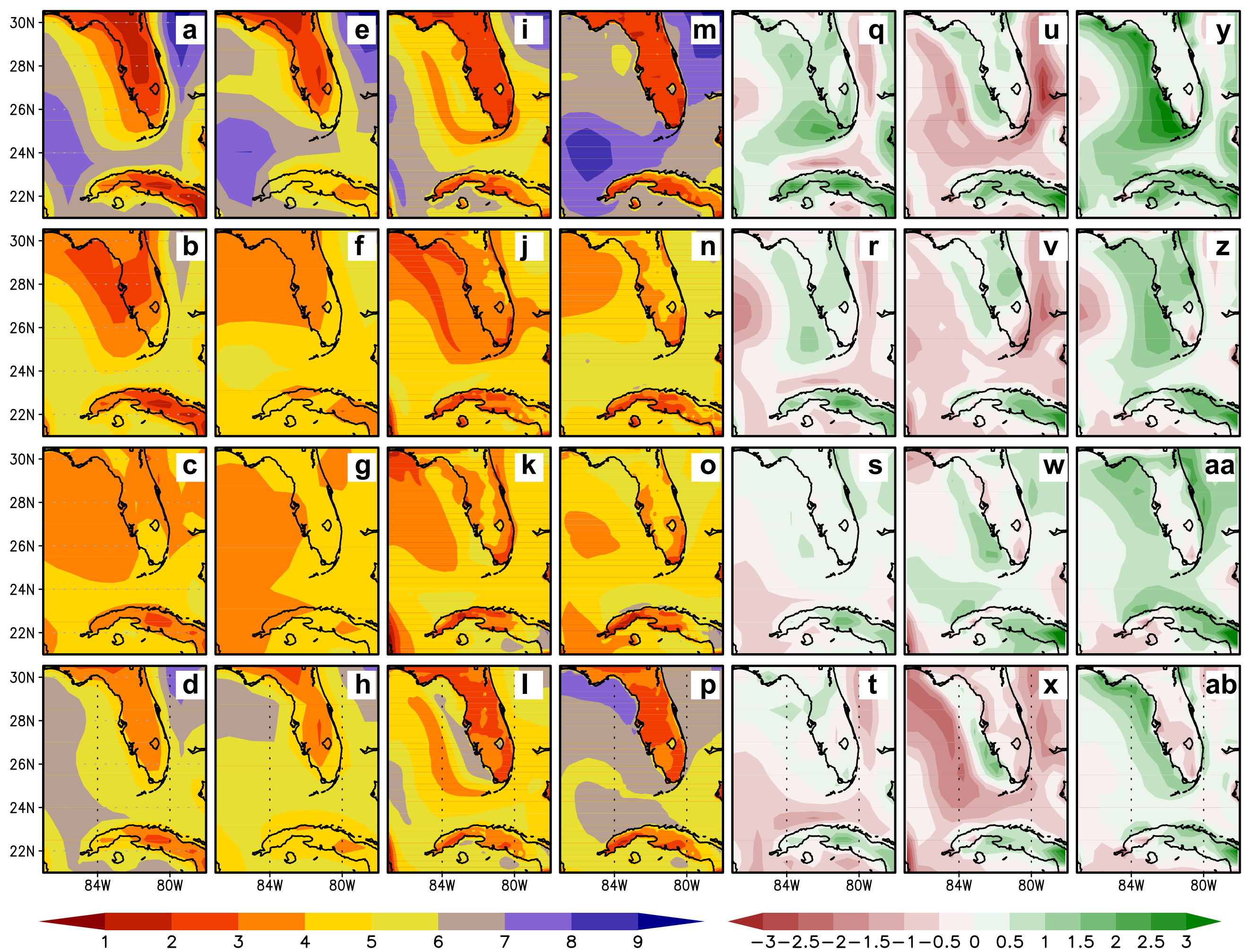

Fig. 4 The climatological seasonal mean surface evaporation from a–d observations, e–h CCSM4, i–l RSMROMS, m–p RSM for a, e, i, m DJF, b, f, j, o MAM, c, g, k, o JJA, and d, h, l, p SON seasons. The corresponding systematic errors from q–t CCSM4, u–x RSMROMS, and y, z, aa, ab RSM for q, u, y DJF, r, v, z MAM, s, w, aa JJA, and t, x, ab SON seasons. The units are in mm day^{-1}

the WFS displayed by RSMROMS relative to RSM suggests the potential benefit of including air-sea coupling.

3.1.3 Surface evaporation

The seasonal cycle of surface evaporation is quite interesting with nearly opposite seasonal cycles over the terrestrial PF and the oceanic WFS regions (Fig. 4a–d). For example, the surface evaporation over PF is weakest (strongest) during the DJF (JJA) season while over the WFS it is strongest (weakest) during the DJF (JJA) season. This is largely because of the reduction in the soil moisture during the dry DJF season over PF which is replenished during the wet JJA season that is critical for surface evaporation over land (Misra et al. 2018). In addition, the surface temperature and downwelling shortwave flux is also comparatively lower in the winter and spring seasons relative to the wet summer season that results in the observed seasonal cycle of terrestrial surface evaporation. Over the oceans, the winds and the boundary layer moisture gradient are stronger during the boreal winter season (not shown), which increases the surface evaporation relative to the summer season. All three models capture this feature of contrasting seasonal cycles of surface evaporation over PF and WFS (Fig. 4e–p). The systematic errors of CCSM4 (Fig. 4q–t) suggest that the evaporative flux is overestimated over the WFS and PF throughout the year. These errors are comparable both over PF and the WFS in CCSM4 (Fig. 4q–t) and RSMROMS (Fig. 4u–x; Table 4). Although, in the RSMROMS simulation there is a strong underestimation of evaporation along the western edge of the WFS throughout the year except in the JJA season. The systematic error of evaporation in RSM is the least in the DJF season (Fig. 4y) and comparatively overestimated in the MAM season (Fig. 4z; Table 4).

The systematic reduction of the RMSE in surface evaporation in RSMROMS compared to RSM across all four seasons (Table 4) yet again reinforces the benefit of air-sea coupling on the simulation of the climate in the region.

3.1.4 Moisture flux convergence

The reanalysis shows a rather dramatic seasonal shift from moisture flux divergence over the WFS and PF in the boreal winter and spring seasons to moisture flux convergence in the summer season before it reverts to divergence over WFS again in the fall season (Fig. 5a–d). This suggests that the seasonal mean precipitation in the seasons of DJF, MAM, and SON over WFS is exclusively sustained by surface evaporation. Our analysis suggests that over PF as well the surface precipitation is exclusively sustained by surface evaporation in DJF (Fig. 5a) and MAM (Fig. 5b) seasons. However, in boreal summer (Fig. 5c) and fall (Fig. 5d) seasons there is additional contribution of moisture flux convergence on surface precipitation over PF. In addition, comparing Figs. 4c and 5c it becomes apparent that surface evaporation dominates over moisture flux convergence both over terrestrial PF and over the WFS during the wet JJA season. All three model simulations show a far less robust seasonal cycle of the moisture flux convergence over both WFS and PF (Fig. 5e-p). For example, the moisture flux divergence prevails over the WFS throughout the year in all three model simulations. Similarly, the shift to moisture flux convergence from divergence over PF in all three model simulations happen in the SON season instead of the observed shift in the JJA season. Furthermore, Table 5 clearly indicates that CCSM4 displays the least RMSE in moisture flux convergence over WFS and PF in most of the seasons except in the JJA season when RSMROMS displays the least. In addition, RSMROMS consistently improves upon RSM with respect to systematic errors of the moisture flux convergence in all seasons except in the DJF and MAM seasons over the WFS (Table 5).

3.1.5 Overall moisture budget

From the discussions in the previous sub-sections it is clear that the precipitation in the winter and spring seasons over the WFS and PF is sustained exclusively by surface evaporation and in the boreal summer season there is some additional contribution from moisture flux convergence. All three models however portray a greater dependence of precipitation on surface evaporation over both WFS and PF especially in the summer season. In terms of the systematic errors in the individual terms of the hydrological budget over PF and WFS, CCSM4 simulation generally shows a higher fidelity than the other two regional model simulations with some exceptions (Fig. 6). In the wet JJA season, however, all three models show comparable fidelity, with RSMROMS showing a modest advantage over the other two models (Fig. 6). The consequence of the relatively coarser resolution of CCSM4 is likely to produce a far smoother field than the finer resolution RSM and RSMROMS simulations, which tend to produce fine scale features. Any dislocation of such mesoscale features in the model simulation is likely to be penalized at verification more severely than not resolving such gradients at all. It may also be noted that the verification data of MERRA-2 is almost five times coarser than either RSM or RSMROMS, which would imply that fine scale features resolved in RSM or RSMROMS may not be necessarily

Table 4 RMSE of evaporation over West Florida Shelf (WFS) and over Peninsular Florida (PF)

	DJF			MAM			JJA			SON		
	CCSM4	RSMROMS	RSM	CCSM4	RSMROMS	RSM	CCSM4	RSMROMS	RSM	CCSM4	RSMROMS	RSM
PF	0.41	0.41	0.47	0.91	0.89	1.03	0.47	0.46	0.49	0.56	0.52	0.68
WFS	0.91	0.89	2.21	0.61	0.60	1.26	0.72	0.70	1.08	0.32	1.25	1.27

Units in mm day^{-1}

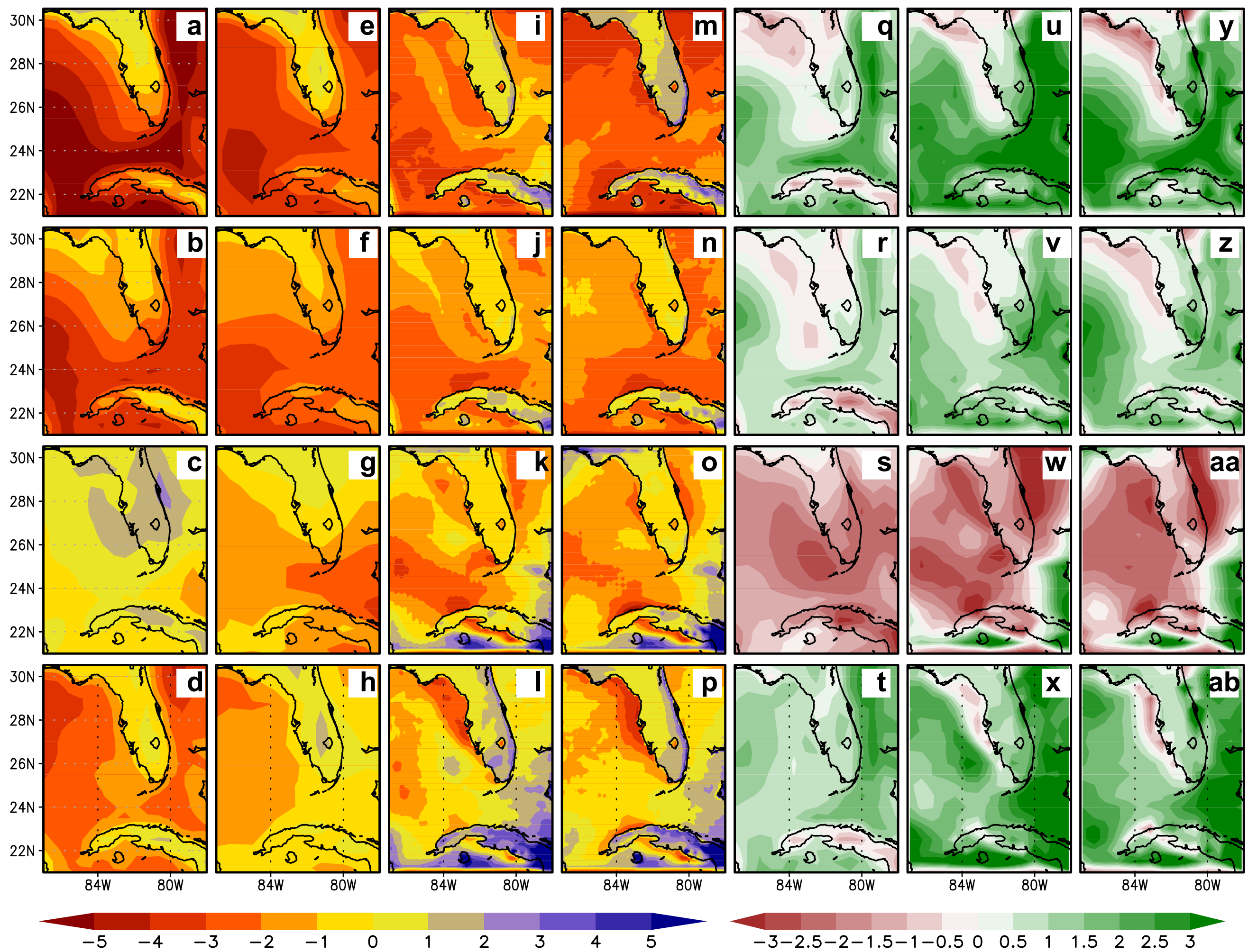

Fig. 5 The climatological seasonal mean moisture flux convergence from a–d observations, e–h CCSM4, i–l RSMROMS, m–p RSM for a, e, i, m DJF, b, f, j, o MAM, c, g, k, o JJA, and d, h, l, p SON seasons. The corresponding systematic errors from q–t CCSM4, u–x RSMROMS, and y–ab RSM for q, u, y DJF; r, v, z MAM, s, w, aa JJA, and t, x, ab SON seasons. The units are in mm day^{-1}

Table 5 RMSE of moisture flux convergence over West Florida Shelf (WFS) and over Peninsular Florida (PF)

	DJF			MAM			JJA			SON		
	CCSM4	RSMROMS	RSM	CCSM4	RSMROMS	RSM	CCSM4	RSMROMS	RSM	CCSM4	RSMROMS	RSM
PF	0.63	1.39	1.77	0.33	1.07	1.16	1.43	1.15	1.51	0.76	1.31	1.26
WFS	0.56	1.39	1.13	0.44	0.72	0.58	2.00	1.89	2.24	0.86	1.67	1.22

Units in mm day^{-1}

resolved in MERRA-2. In Fig. 6, it may be noted that systematic errors of surface precipitation and evaporation are quite comparable in CCSM4 and RSMROMS over both the WFS and PF. The largest differences between the two model simulations over these two regions are in with reference to the moisture flux convergence (Fig. 6). Therefore, it may be noted that despite the limitations of the coarse resolution of the verification data, it is revealing that RSMROMS displays a higher fidelity in the components of the moisture budget than RSM with very few exceptions (Fig. 6), which suggests the potential role of the rectification impact of air-sea coupling on the regional model simulations.

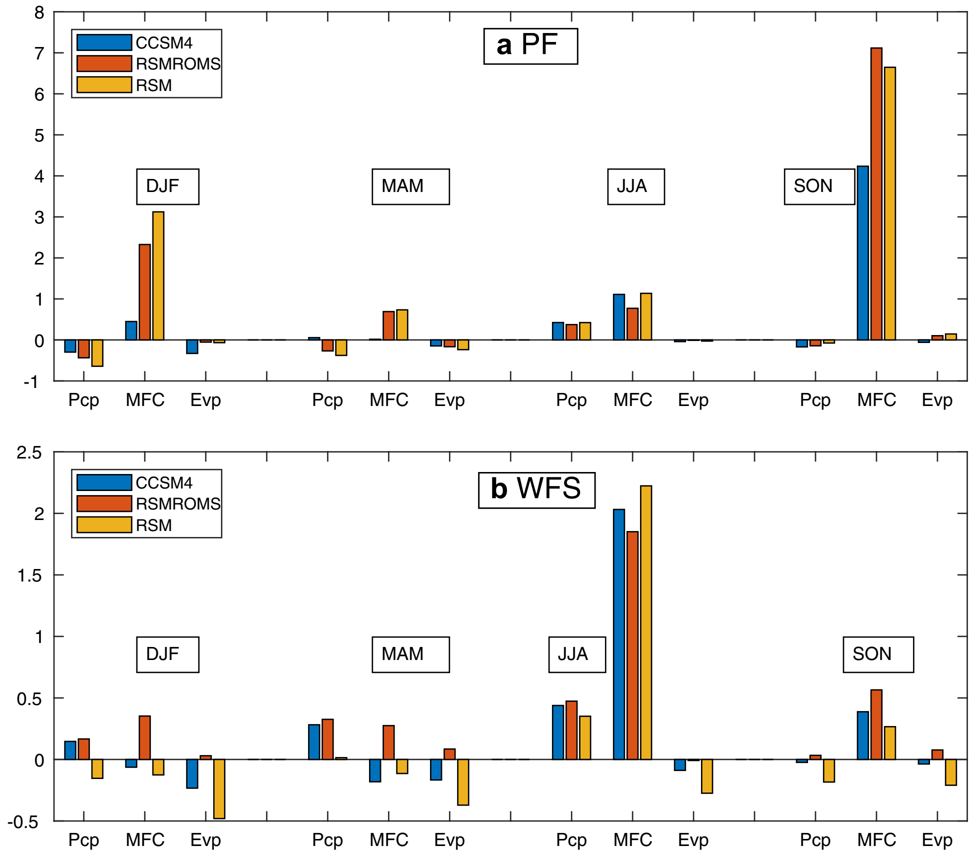

Fig. 6 Systematic errors of precipitation *pcp*, moisture flux convergence (MFC), and surface evaporation *Evp* for the four seasons over **a** PF and **b** WFS. The units are in mm day^{-1}

3.2 Simulation of the future climate (2041–2060)

In this section, we discuss the future climate projections from these models after having analyzed the fidelity and limitations of the models for its current climate simulation in the previous sub-sections.

The CCSM4 future projection in Fig. 7a–d shows insignificant change in precipitation over PF and the WFS throughout the year except in JJA season when there is a slight drying tendency (<0.5 mm day^{-1}) in central and south Florida parts of southwestern WFS (Fig. 7c). The future projection of the seasonal rainfall in RSMROMS (Fig. 7e–h) indicate that there is significant drying projected over PF in the JJA season with south Florida displaying over 1 mm day^{-1} drying. In contrast, the projections of RSM (Fig. 7i-l) suggest that the drying over PF in the JJA season is statistically insignificant, while changes in precipitation over the WFS in all four seasons are statistically significant. These changes in precipitation are also marked by similar changes in moisture flux convergence and surface evaporation (not shown). For example, the projected drying over PF in JJA season in CCSM4 (Fig. 7c) is consistent with corresponding projected reduction in moisture flux convergence (Fig. 8a) and relatively lower reduction in surface evaporation (Fig. 8d). However, in RSMROMS the projected drying over PF in JJA (Fig. 7g) is sustained by a larger projected reduction in surface evaporation (Fig. 8e) and comparatively lower projected reduction in moisture flux convergence (Fig. 8b). In the RSM the projected change of precipitation over PF in JJA is barely significant (Fig. 7k).

Despite the insignificant changes to the future hydroclimate of the WFS and PF in the rest of the year except in the JJA season, there is significant and consistent warming throughout the year in the projected SST over the WFS in both CCSM4 and RSMROMS (Fig. 9). The biggest difference in the projected SST between the two models is that the largest changes are oriented along the WFS in RSMROMS while in CCSM4 the changes are more zonal. This pattern of warm SST over WFS in RSMROMS stems from slowing of the Loop Current in the future climate (not shown) and improved resolution of the bathymetry which makes the ocean shallower and respond to changes in the atmospheric fluxes. In oceanic downscaling of many GCM projections, Liu et al. (2012, 2015) also indicated significant deceleration of the Loop Current, that resulted in a net ocean heat flux from the warm Caribbean Sea in to the Gulf of Mexico.

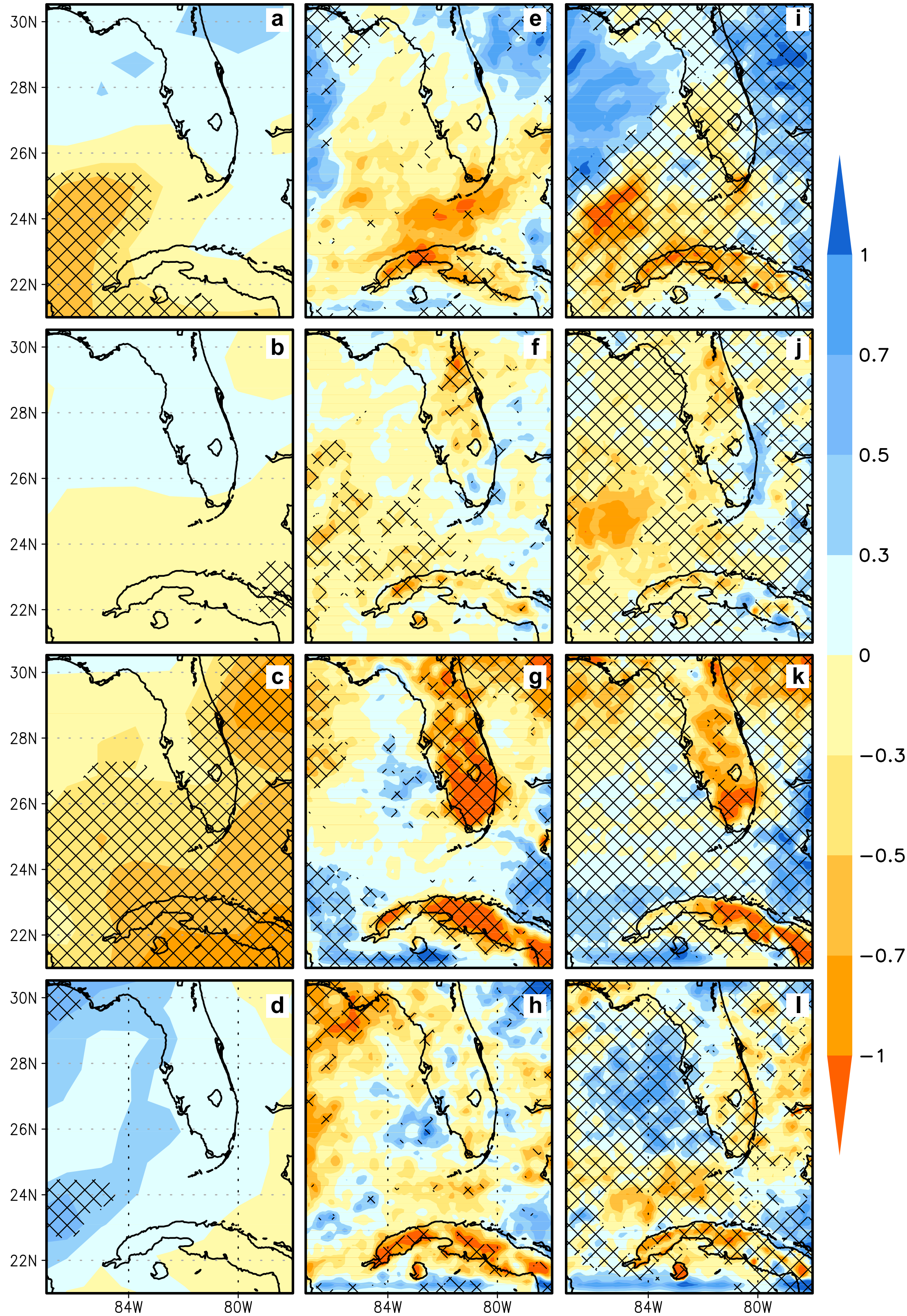
a
b
c
d
e
f
g
h
i
j
k
l
30N
28N
26N
24N
22N
84W
80W
1
0.7
0.5
0.3
0
−0.3
−0.5
−0.7
−1

◂**Fig. 7** The projected (2041–2060) climatological seasonal mean difference of precipitation from the corresponding climatological seasonal mean of the current climate (1986–2005) from **a–d** CCSM4, **e–h** RSMROMS and **i–l** RSM for **a, e, i** DJF; **b, f, j** MAM; **c, g, k** JJA; and **d, h, l** SON seasons. The hashed regions are statistically significant at 90% confidence interval according to t-test. The units are in mm day^{-1}

4 Discussion and conclusions

This is one of the unique studies over Florida that has attempted to compare coupled ocean–atmosphere and uncoupled regional climate downscaling projections besides comparing it with the coarse GCM driving the regional models. Traditionally, DD has been conducted in reduced systems with either atmosphere only or ocean only models that have relatively higher resolution than their driving GCMs. This comparative analysis is important for a region like PF, which is poorly resolved in several of the coarse GCMs and is surrounded by oceans with robust surface ocean currents and broad continental shelf. The downscaling to 10 km grid spacing in this study clearly shows the advantage in resolving the coastlines, the topography over PF, and the bathymetry in the surrounding oceans to be far more realistic than its crude rendition in a GCM like the CCSM4.

The validation of the two decades of the twentieth century simulation does indicate that the fidelity of CCSM4 in terms of the systematic errors of the seasonal mean variables of the hydroclimate is difficult to overcome in either coupled or uncoupled atmospheric downscaling despite having improved simulations of the SST in RSMROMS. This can be a result of the lateral boundary forcing from an imperfect driving GCM and the quality of the regional model itself (Misra and Kanamitsu 2004; Rummukainen 2010; Feser et al. 2011). The comparison of RSMROMS with CCSM4 however, showed the benefit of higher resolution in RSMROMS in resolving the ocean bathymetry in the WFS that resulted in improved simulation of the seasonal SST.

In this study, a unique opportunity arises to assess the potential rectification effect of air-sea coupling on the regional simulation by comparing RSMROMS with RSM driven by the same GCM (CCSM4). This comparison shows that for a majority of the seasons, RSMROMS has a lower systematic error of the seasonal mean precipitation, surface evaporation and moisture flux convergence over the WFS and PF compared to RSM. This clearly demonstrates the impact of air-sea coupling in potentially rectifying some of the systematic errors of RSM. We have chosen the highest resolution and the latest global atmospheric reanalysis of MERRA2 for validation of the moisture budget variables. However, it may be pointed that MERRA2 is still about five times coarser than the 10 km grid resolution of either RSM or RSMROMS. Therefore, in this comparison it is quite possible that the RSM and the RSMROMS are being unfairly penalized for producing features that are potentially unresolved in MERRA2. Notwithstanding these limitations in MERRA2, our analysis reveals that RSMROMS displays the least RMSE in the components of the moisture budget in the wet JJA season relative to the other two models. This result reinforces the benefit of using high-resolution coupled ocean–atmosphere models for simulating the wet season climate over the region, when precipitation is strongly influenced by local forcing.

In terms of the climate projection in the decades of 2041–2060, the RSMROMS simulation indicate significant drying over PF in JJA season relative to moderate drying in CCSM4, which is contrary to the RSM simulation that suggests insignificant changes to seasonal precipitation. This projected change in summer season precipitation in RSMROMS and CCSM4 is associated with corresponding decrease in surface evaporation and comparatively smaller reduction in moisture convergence. Another significant difference in the projections between CCSM4 and RSMROMS is that of SST, especially over the WFS. The projected warming of SST in CCSM4 is more zonally oriented as opposed to be along the WFS in RSMROMS. This latter structure is likely a result of the more realistic bathymetry of the WFS in RSMROMS and the slowing of the Loop Current in a future warm climate.

The clear difference in the projections of the surface climate over WFS between RSMROMS and CCSM4 seems to be a result of resolving the shallower bathymetry of WFS in RSMROMS. Similarly, the differences in the projections of the surface hydroclimate over PF across the simulations of CCSM4, RSM, RSMROMS highlight the importance of both resolution and air-sea coupling. We therefore believe that the expansion of this study with more such downscaled integrations with coupled ocean–atmosphere regional models to encompass the various uncertainties stemming from internal variations of the climate, emission scenarios, and GCMs is imperative.

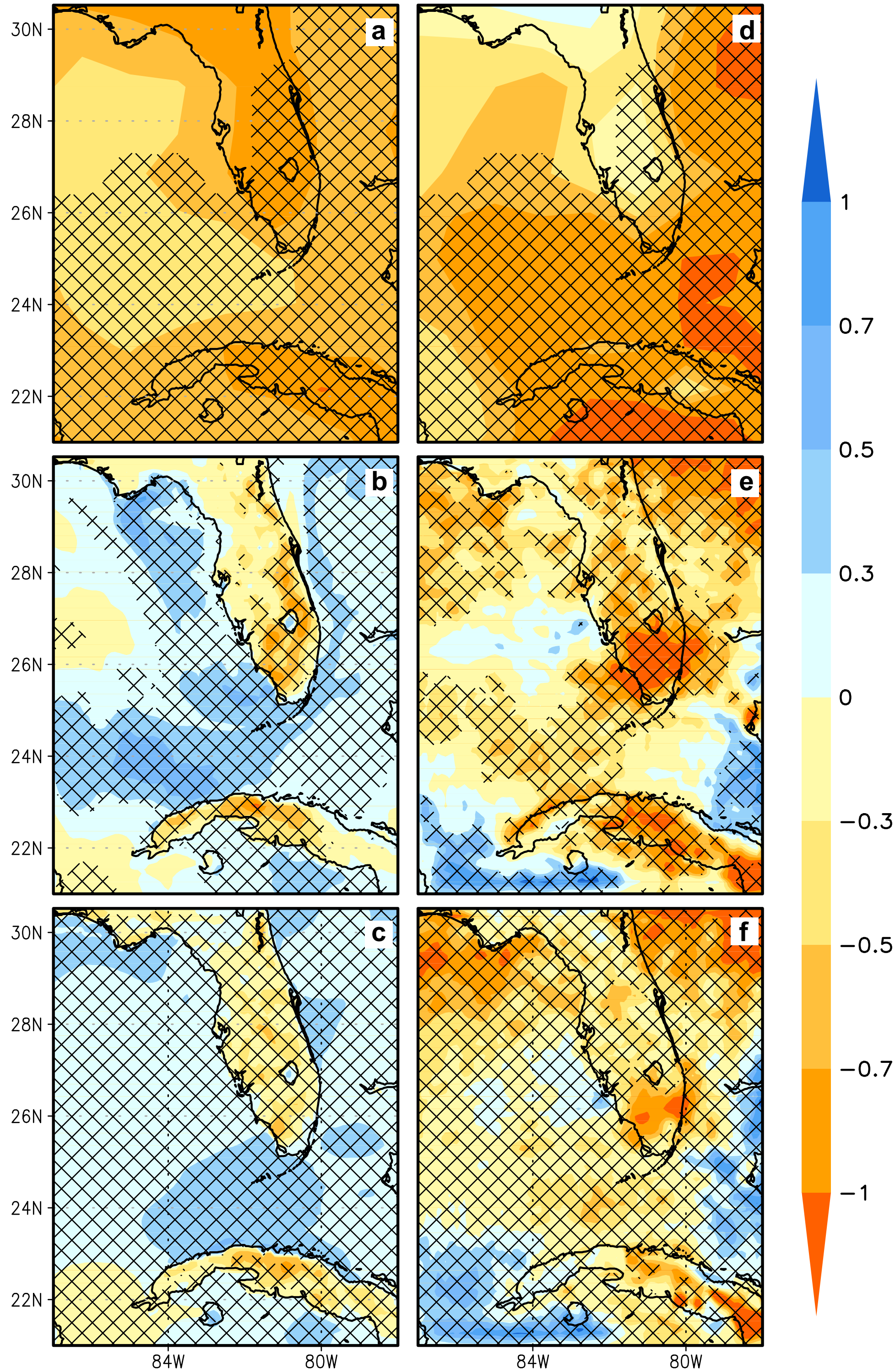

Fig. 8 The difference in the projected (2041–2060) climatological JJA seasonal mean from the corresponding climatological seasonal mean of the current climate (1986–2005) of **a**–c moisture flux convergence and **d**–**f** surface evaporation from **a, d** CCSM4, **b, e** RSMROMS and **c, f** RSM. The hashed regions are statistically significant at 90% confidence interval according to t-test. The units are in mm day^{-1}

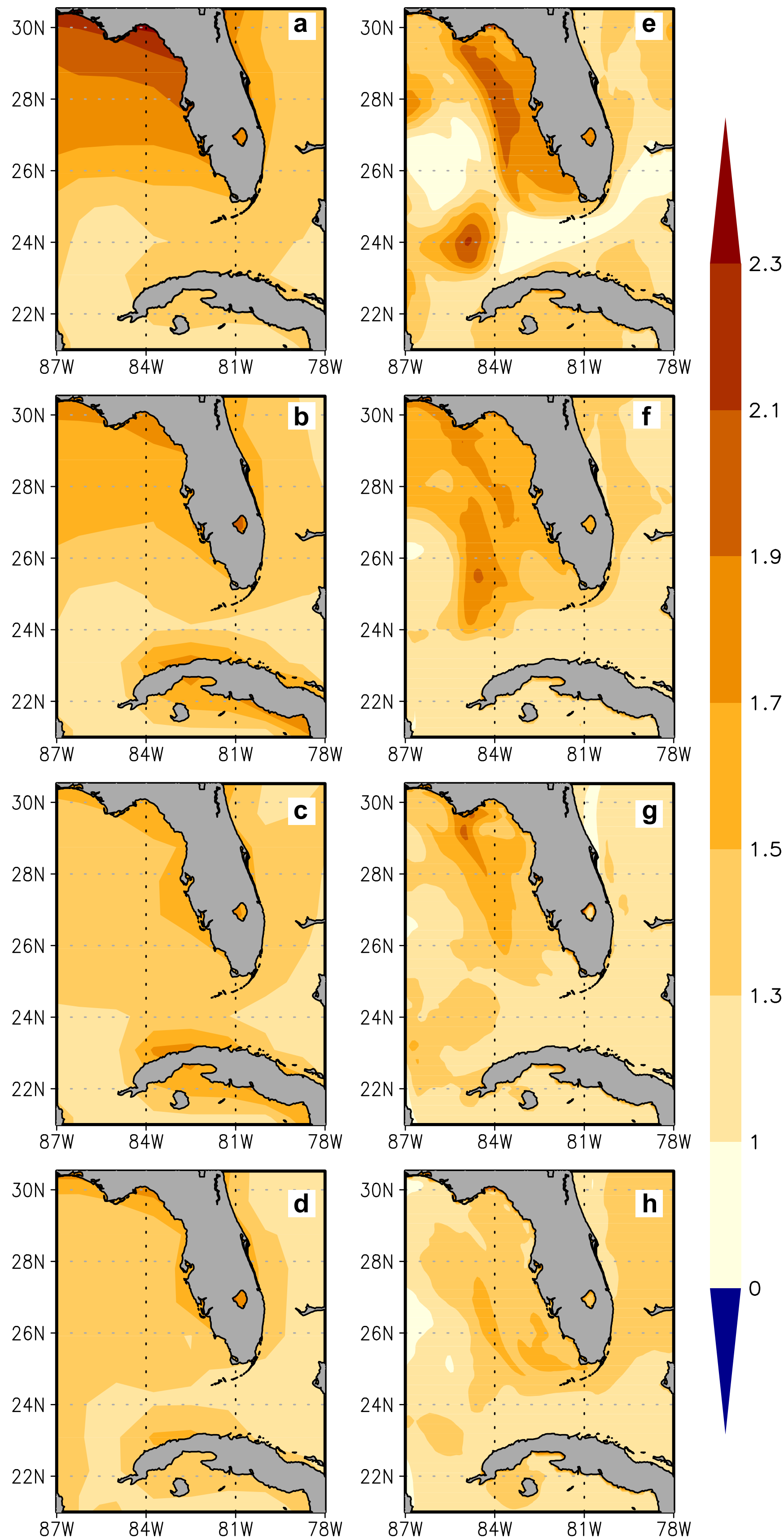

Fig. 9 The projected (2041–2060) seasonal mean climatological difference from the corresponding mean seasonal current climate (1986–2005) from **a–d** CCSM4, **e–h** RSM-ROMS for SST (°C) for **a, e** DJF, **b, f** MAM, **c, g** JJA, and **d, h** SON seasons. All the shaded regions are statistically significant at 90% confidence interval according to *t* test

Acknowledgements This work was supported by NOAA grant NA12OAR4310078 and the South Florida Water Management District (PO 039231). The authors have no conflicts of interest to declare.

References

Adler RF, Huffman GJ, Bolvin DT, Curtis S, Nelkin EJ (2000) Tropical rainfall distributions determined using TRMM combined with other satellite and rain gauge information. J Appl Meteorol 39(12):2007–2023

Alpert J, Kanamitsu M, Caplan P, Sela J, White G (1988) Mountain induced gravity wave drag parameterization in the NMC medium-range forecast model. In Conference on Numerical Weather Prediction, 8th, Baltimore, MD. 726–733

Boyer TP, Stephens C, Antonov JI, Conkright ME, Locarnini LA, O'Brien TD, Garcia HE (2002) Salinity. NOAA Atlas NESDIS 49 2:165 pp World Ocean Atlas 2001

Carlson E (2012) Population trends in Florida, 2000 to 2030. In Climate Scenarios: A Florida-Centric View, ed. V. Misra, Available from:http://floridaclimate.org/climate_scenario_pdf.php

Carton JA, Giese BS (2008) A reanalysis of ocean climate using Simple Ocean Data Assimilation (SODA). Mon Weather Rev 136(8):2999–3017

Chan S, Misra V (2011) Dynamic downscaling of the North American with the ECPC-NCEP Regional Spectral Model from NCEP CFS global model-varied representation. J Climate 24:653–673

Chang YL, Oey LY (2010) Why can wind delay the shedding of Loop Current eddies? J Phys Oceanogr 40(11):2481–2495

Chou MD, Lee KT (1996) Parameterizations for the absorption of solar radiation by water vapor and ozone. J Atmos Sci 53:1203–1208

Chou MD, Lee KT, Tsay SC, Fu Q (1999) Parameterization for cloud longwave scattering for use in atmospheric models. J Clim 12(1):159–169

Dixon LK, Kirkpatrick GJ, Hall ER, Nissanka A (2014) Nitrogen, Phosphorous, and Silica on the west Florida shelf: patterns and relationships with Karenia spp. Occurrence Harmful Algae 38:8–19. https://doi.org/10.1016/j.hal.2014.07.001

Ek MB, Mitchell KE, Lin Y, Rogers E, Grunmann P, Koren V, Gayno G, Tarpley JD (2003) Implementation of Noah land surface model advances in the National Centers for Environmental Prediction operational mesoscale Eta model. J Geophys Res 108:22

Feser F, Burkhardt R, von Storch H, Winterfeldt J, Zahn M (2011) Regional climate models add value to global model data. Bull Am Soc. https://doi.org/10.1175/2011BAMS3061.1

Gent PR, Danabasoglu G, Donner LJ, Holland MM, Hunke EC, Jayne SR, Lawrence DM, Neale RB, Rasch PJ, Vertenstein M, Worley PH (2011) The community climate system model version 4. J Clim 24(19):4973–4991

Giorgi F, Gutowski WJ Jr (2015) Regional dynamical downscaling and the CORDEX initiative. Annu Rev Environ Resour 40:467–490

Haidvogel DB, Arango HG, Hedstrom K, Beckmann A, Malanotte-Rizzoli P, Shchepetkin AF (2000) Model evaluation experiments in the North Atlantic Basin: simulations in nonlinear terrain-following coordinates. Dynam Atmos Oceans 32(3):239–281

He R, Weisberg RH, Zhang H, Muller-Karger FE, Helber RW (2003) A cloud free, satellite derived, sea surface temperature analysis for the West Florida Shelf. Geophys Res Lett. https://doi.org/10.1029/2003GL017673

Heil CA, Bronk DA, Dixon LK, Hitchcock L et al (2014) The Gulf of Mexico (ECOHAB): Karenia program 2006–2012. Harmful Algae 38:3–7. https://doi.org/10.1016/j.hal.2014.07.015

Hewitson BC, Crane RG (1996) Climate downscaling: techniques and application. Clim Res 5:85–95

Hong SY, Pan HL (1996) Nonlocal boundary layer vertical diffusion in a medium-range forecast model. Mon Weather Rev 124(10):2322–2339

Huffman GJ, Adler RF, Rudolf B, Schneider U, Keehn PR (1995) Global precipitation estimates based on a technique for combining satellite-based estimates, rain gauge analysis, and NWP model precipitation information. J Clim 8(5):1284–1295

Huffman GJ, Adler RF, Arkin P, Chang A, Ferraro R, Gruber A, Janowiak J, McNab A, Rudolf B, Schneider U (1997) The global precipitation climatology project (GPCP) combined precipitation dataset. Bull Am Meteor Soc 78(1):5–20

Juang HM, Kanamitsu M (1994) The NMC nested regional spectral model. Mon Weather Rev 122:3–26

Kanamitsu M, Yoshimura K, Yhang YB, Hong SY (2010) Errors of interannual variability and trend in dynamical downscaling of reanalysis. J Geophys Res 115:17

Kirtman B, Bitz C, Bryan F et al (2012) Impact of ocean model resolution on CCSM climate simulations. Clim Dyn 39:1303–1328. https://doi.org/10.1007/s00382-012-1500-3

Kirtman BP, Perlin N, Siqueira L (2017) Ocean eddies and climate predictability. Chaos Interdiscip J Nonlinear Sci 27:126902. https://doi.org/10.1063/1.4990034

Large WG, McWilliams JC, Doney SC (1994) Oceanic vertical mixing: a review and a model with a nonlocal boundary layer parameterization. Rev Geophys 32(4):363–403

Laurindo LC, Siqueira L, Mariano AJ, Kirtman BP (2018) Cross-spectral analysis of the SST/10-m wind speed coupling resolved by satellite products and climate model simulations. Clim Dyn Submitt

Li H, Kanamitsu M, Hong SY (2012) California reanalysis downscaling at 10 km using an ocean -atmosphere coupled regional model system. J Geophys Res 117:12

Liu Y, Weisberg RH (2012) Seasonal variability on the West Florida Shelf. Prog Oceanogr 104:80–98

Liu Y, Lee SK, Muhling BA, Lamkin JT, Enfield DB (2012) Significant reduction of the loop current in the 21st century and its impact on the Gulf of Mexico. J Geophys Res 117:C05039. https://doi.org/10.1029/2011JC007555

Liu H, Wang C, Lee SK, Enfield DB (2013) Atlantic warm pool variability in the CMIP5 simulations. J Clim 26:5315–5336. https://doi.org/10.1175/JCLI-D-12-00556.1

Liu Y, Lee SK, Enfield DB, Muhling BA, Lamkin JT, Muller-Karger FE, Roffer MA (2015) Potential impact of climate change on the intra-Americas Sea: part-1. A dynamic downscaling of the CMIP5 model projections. J Mar Syst 148:56–69

Mellor GL, Yamada T (1982) Development of a turbulence closure model for geophysical fluid problems. Rev Geophys 20(4):851–875

Misra V (2005) Simulation of the intraseasonal variance of the South American summer monsoon. Mon Weather Rev 133(3):663–676

Misra V, Dirmeyer PA (2009) Air, sea, and land interactions of the continental US hydroclimate. J Hydrometeorol 10(2):353–373

Misra V, Kanamitsu M (2004) Anomaly Nesting: a methodology to dowscale seasonal climate climate simulations from an AGCM. J Clim 17:3249–3262

Misra V, Mishra A (2016) The oceanic influence on the rainy season of Peninsular Florida. J Geophys Res 121(13):7691–7709

Misra V, DiNapoli S, Bastola S (2013) Dynamic downscaling of the 20th century reanalysis over the southeastern United States. Reg Env Change 13:15–23. https://doi.org/10.1007/s00382-012-0372-8

Misra V, Mishra A, Li H (2016) The sensitivity of the regional coupled ocean-atmosphere simulations over the Intra-Americas seas to the prescribed bathymetry. Dynam Atmos Oceans 76:29–51

Misra V, Mishra A, Bhardwaj A (2017) High -resolution regional -coupled ocean–atmosphere simulation of the Indian Summer Monsoon. Int J Climatol. https://doi.org/10.1002/joc5034

Misra V, Mishra A, Bhardwaj A, Viswanathan K, Schmutz D (2018) The potential role of land cover on secular changes of the hydroclimate of Peninsular Florida. NPJ Clim Atmos Sci. https://doi.org/10.1038/s41612-018-0016-x

Moorthi S, Suarez MJ (1992) Relaxed Arakawa-Schubert. A parameterization of moist convection for general circulation models. Mon Weather Rev 120(6):978–1002

Rummukainen M (2010) State-of-the-art with regional climate models. WIREs Clim Change 1:82–96

Shchepetkin AF, McWilliams JC (2005) The regional oceanic modeling system (ROMS): a split-explicit, free-surface, topography-following-coordinate oceanic model. Ocean Modelling 9(4):347–404

Shukla J, Hagedorn R, Hoskins B, Kinter J, Marotzke J, Miller M, Palmer TN, Slingo J (2009) Revolution in climate prediction is both necessary and possible: a declaration at the world modelling summit for climate prediction. Bull Am Meteol Soc 2:175–178

Siqueira L, Kirtman BP (2016) Atlantic near-term climate variability and the role of a resolved Gulf Stream. Geophys Res Lett 43:3964–3972. https://doi.org/10.1002/2016GL068694

Smith SK (2005) Florida Population Growth: Past, Present and Future. Research Report by the Bureau of Economic and Business Research, University of Florida. Retrieved from: https://www.bebr.ufl.edu/sites/default/files/Research%20Reports/FloridaPop2005_0.pdf

Steidinger KA (1975) Basic factors influencing red tides. Florida Department of Natural Resources Marine Research Laboratory, 153–162

Suarez M, Bacmeister J (2015) Development of the GEOS-5 atmospheric general circulation model: evolution from MERRA to MERRA2. Geosci. Model Dev 8:1339–1356. https://doi.org/10.5194/gmd-8-1339-2015

Tatsumi Y (1986) A spectral limited area model with time dependent lateral boundary conditions and its application to a multi-level primitive equation model. J Meteor Soc Japan 64:637–663

Tiedtke M (1983) The sensitivity of the time-mean large-scale flow to cumulus convection in the ECMWF model. In: Proceedings of ECMWF Workshop on Convective in Large-scale Models. European Centre for Medium-Range Weather Forecasts, Reading, United Kingdom. 297–316

Tolbert WH, Salsman GG (1964) Surface circulation of the eastern Gulf of Mexico as determined by drift bottled studies. J Geophys Res 69:223–230

Umlauf L, Burchard H (2003) A generic length-scale equation for geophysical turbulence models. J Mar Res 61(2):235–265

van Vuuren DP, Edmonds JA, Kainuma M et al (2011) A special issue on the RCPs. Clim Change 109:1–4. https://doi.org/10.1007/s10584-011-0157-y

Weisberg RH, He R, Kirkpatrick G, Muller-Karger F, Walsh JJ (2004) A West Florida Shelf case study: coastal ocean circulation on remotely sensed, Oceanography, 70–75

Weisberg RH, Zheng L, Liu Y (2016a) West Florida shelf upwelling: Origins and pathways. J Geophys Res Oceans 121:5672–5681. https://doi.org/10.1002/2015JC011384

Weisberg RH, Zheng L, Liu Y (2016b) West Florida shelf upwelling: Origins and pathways. J Geophys Res (oceans) 121:56772–5681

Wilby RL, Wigley TM (1997) Downscaling general circulation model output: a review of methods and limitations. Prog Phys Geogr 21(4):530–548

Wilks D (2011) Statistical methods in the atmospheric sciences. 3rd edn, Int Geophys Ser 100: 704 pp

Yang H, Weisberg RH (1999) West Florida continental shelf circulation response to climatological wind forcing. J Geophys Res 104:5301–5320

Zhao Q, Carr FH (1997) A prognostic cloud scheme for operational NWP models. Mon Weather Rev 125(8):1931–1953

(2014) The Gulf of Mexico ECOHAB: Karenia Program 2006–2012, Harmful Algae, 38, 3–7, https://doi.org/10.1016/j.hal.2014.07.015